

# Sensitivity-Enhanced Static $^{15}\text{N}$ NMR of Solids by $^1\text{H}$ Indirect Detection

Mei Hong and Satoru Yamaguchi

Department of Chemistry, Iowa State University, Ames, Iowa 50011

Received October 16, 2000; revised February 13, 2001; published online April 17, 2001

**A method for enhancing the sensitivity of  $^{15}\text{N}$  spectra of nonspinning solids through  $^1\text{H}$  indirect detection is introduced. By sampling the  $^1\text{H}$  signals in the windows of a pulsed spin-lock sequence, high-sensitivity  $^1\text{H}$  spectra can be obtained in two-dimensional (2D) spectra whose indirect dimension yields the  $^{15}\text{N}$  chemical shift pattern. By sacrificing the  $^1\text{H}$  chemical shift information, sensitivity gains of 1.8 to 2.5 for the  $^{15}\text{N}$  spectra were achieved experimentally. A similar sensitivity enhancement was also obtained for 2D  $^{15}\text{N}$ - $^1\text{H}$  dipolar and  $^{15}\text{N}$  chemical shift correlation spectroscopy, by means of a 3D  $^1\text{H}/^{15}\text{N}$ - $^1\text{H}/^{15}\text{N}$  correlation experiment. We demonstrate this technique, termed PRINS for proton indirectly detected nitrogen static NMR, on a crystalline model compound with long  $^1\text{H}$   $T_{1\rho}$  and on a 25-kDa protein with short  $^1\text{H}$   $T_{1\rho}$ . This  $^1\text{H}$  indirect detection approach should be useful for enhancing the sensitivity of  $^{15}\text{N}$  NMR of oriented membrane peptides. It can also be used to facilitate the empirical optimization of  $^{15}\text{N}$ -detected experiments where the inherent sensitivity of the sample is low.** © 2001 Academic Press

**Key Words:** sensitivity enhancement; pulse spin-lock sequence; indirect detection; separated local field spectroscopy;  $^{15}\text{N}$  static NMR.

## INTRODUCTION

$^1\text{H}$  indirect detection is commonly used in solution NMR to enhance the sensitivity of heteronuclear spectra (1). Recently, this approach was also introduced to solid-state  $^{15}\text{N}$  experiments where the samples undergo fast magic-angle spinning (2). A sensitivity enhancement factor of 2.0 to 3.2 was observed experimentally. The enhancement relied on the ability to narrow the  $^1\text{H}$  lines significantly, even for rigid solids, by using spinning speeds of about 30 kHz.

While MAS experiments are clearly important for site-resolved studies of solids, static  $^{15}\text{N}$  NMR has found an important application in the structural investigations of peptides and proteins immobilized in lipid bilayers (3, 4). The sensitivity of the  $^{15}\text{N}$  spectra of these membrane peptides is usually low, due to the limited amount of isotopically labeled samples available. Therefore, it is of interest to improve the sensitivity of static  $^{15}\text{N}$  spectra through  $^1\text{H}$  indirect detection. To achieve sensitivity gains, the linewidths of the  $^1\text{H}$  spectra must be small. Without sample spinning, the only practical way to achieve this is to employ a pulsed spin-lock detection scheme. This technique, demonstrated recently for  $^2\text{H}$  NMR (5), involves detecting the

$^1\text{H}$  signals in the windows of a multiple-pulse train whose pulse phase is along the magnetization direction (Fig. 1). The  $^1\text{H}$  signals decay with the rotating frame spin-lattice relaxation time,  $T_{1\rho,\text{H}}$  (6). Fourier transformation of the exponential decay yields a single  $^1\text{H}$  peak at the zero frequency of the spectrum, the intensity of which equals the integrated intensities of the time signal. Since no  $^1\text{H}$  chemical shift dispersion is detected, the  $^{15}\text{N}$  spectrum is contained in a single cross section at the center of the  $^1\text{H}$  spectral dimension. Therefore, increased  $^{15}\text{N}$  sensitivity can be achieved at the expense of  $^1\text{H}$  site resolution, as the latter is irrelevant for the purpose of obtaining sensitivity-enhanced  $^{15}\text{N}$  spectra. We show here that the width of this  $^1\text{H}$  zero-frequency peak is sufficiently small for typical crystalline solids and proteins to make sensitivity enhancements over direct  $^{15}\text{N}$  detection possible. For convenience, we call this technique PRINS, which stands for proton indirectly detected nitrogen static NMR.

Two PRINS pulse sequences, one for the 2D  $^1\text{H}$ -detected  $^{15}\text{N}$  experiment and the other for a 3D  $^1\text{H}$ -detected  $^{15}\text{N}$ - $^1\text{H}$  dipolar and  $^{15}\text{N}$  chemical shift correlation experiment, are shown in Fig. 1. In both sequences, cross polarization (CP) is used to transfer the magnetization from  $^1\text{H}$  to  $^{15}\text{N}$  and back. Sensitive detection of the  $^{15}\text{N}$  chemical shift spectrum is achieved by changing the phase of the second  $^{15}\text{N}$  CP pulse. A  $z$ -filter after the first CP removes the direct  $^1\text{H}$  magnetization that was not transferred from the  $^{15}\text{N}$  spins. The  $^1\text{H}$  pulse length in the multiple-pulse train is optimized to be shorter than the  $90^\circ$  pulse length, as it has been shown that a smaller flip angle increases the decay constants, thereby increasing the intensity of the  $^1\text{H}$  zero-frequency peak (6).

The PRINS technique can be extended to enhance the sensitivity of 2D dipolar chemical-shift correlation spectroscopy, which is traditionally performed with heteronuclear detection. By appending the  $^{15}\text{N}$ -to- $^1\text{H}$  polarization transfer and the  $^1\text{H}$  pulsed spin-lock detection to the end of a standard separated-local-field (SLF) sequence (7, 8), we obtain a  $^1\text{H}$ -detected 3D SLF experiment, the theoretical sensitivity enhancement factor of which is the same as that for the 2D experiment in sequence (a).

We can estimate the sensitivity enhancement due to this  $^1\text{H}$  pulsed spin-lock detection in a similar manner to that shown in Refs. (2, 9). Factors that increase the sensitivity of  $^1\text{H}$  detection include the higher gyromagnetic ratio ( $\gamma$ ) of  $^1\text{H}$ , the higher quality factor ( $Q$ ) of the radiofrequency (RF) coil for  $^1\text{H}$  detection,

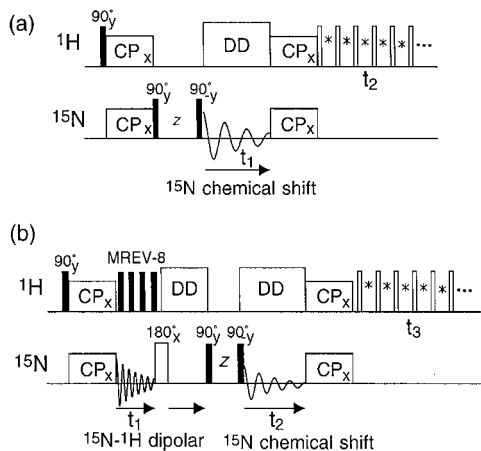


**FIG. 1.** PRINS pulse sequences used in this work. (a) 2D  $^1\text{H}$  indirectly detected  $^{15}\text{N}$  experiment. (b) 3D  $^1\text{H}$  indirectly detected  $^{15}\text{N}$ - $^1\text{H}$  dipolar and  $^{15}\text{N}$  chemical shift correlation experiment. The  $^1\text{H}$  time signal is detected during the windows of the multiple-pulse train. Typical pulses of  $2\text{-}\mu\text{s}$  duration and windows of about  $9\text{ }\mu\text{s}$  were used in the spin-lock train.

and the longer decay constant ( $T_{1\rho,\text{H}}$ ) of  $^1\text{H}$  due to the pulsed spin-lock detection. Factors that reduce the sensitivity gain by  $^1\text{H}$  detection include the less-than-unity cross-polarization ( $10$ ) efficiency ( $f$ ), the frequency discrimination of the indirect dimension necessary for 2D acquisition, and the increased  $^1\text{H}$  noise due to the use of a larger  $^1\text{H}$  filter width ( $\text{FW}_{\text{H}}$ ) than the spectral width ( $\text{SW}_{\text{H}}$ ), which is necessitated by detection in the windows of the multiple-pulse sequence. The key sample-dependent parameters that determine the degree of sensitivity enhancement are the decay constants of the  $^1\text{H}$  ( $T_{1\rho,\text{H}}$ ) and  $^{15}\text{N}$  ( $T_{\text{X, aq}}$ ) signals. Combining these factors, the PRINS enhancement factor  $\xi$  can be written as

$$\xi = \frac{f}{2\sqrt{2}} \cdot \left(\frac{\gamma_{\text{H}}}{\gamma_{\text{X}}}\right)^{3/2} \left(\frac{Q_{\text{H}}}{Q_{\text{X}}}\right)^{1/2} \left(\frac{\eta_{\text{H}}}{\eta_{\text{X}}}\right) \left(\frac{\text{SW}_{\text{H}}}{\text{FW}_{\text{H}}}\right)^{1/2} \left(\frac{T_{1\rho,\text{H}}}{T_{\text{X, aq}}}\right)^{1/2}. \quad [1]$$

For  $^1\text{H}$ -detected  $^{15}\text{N}$  NMR, the gyromagnetic ratios contribute a factor of 31.6 to the sensitivity gain. For a double-resonance probe, the  $^1\text{H}$   $Q$ -factor is typically about twice the  $^{15}\text{N}$   $Q$ -factor. The electronic filling factor of the  $^1\text{H}$  channel ( $\eta_{\text{H}}$ ) for the Bruker probe used in this work is lower than that of the  $X$  channel ( $\eta_{\text{X}}$ ), based on information provided by the manufacturer. We assume a factor of 2 reduction in  $\eta_{\text{H}}$  compared to  $\eta_{\text{X}}$ . The less-than-unity CP efficiency results from both rotating-frame spin-lattice relaxation effects and the fact that the equilibrium  $^1\text{H}$  magnetization of an  $\text{N-H}^{\text{N}}\text{-H}^{\alpha}$  spin system in a peptide after the second cross polarization is about 67% of the  $^{15}\text{N}$  magnetization that would be detected in a direct  $^{15}\text{N}$  experiment. We estimate an overall CP efficiency of 0.5. The larger  $^1\text{H}$  filter width contributes a sensitivity reduction of a factor of 2.5, if a 625-kHz filter width and a 100-kHz spectral width are used, which is the case in our

experiments. Combining these factors, we obtain

$$\xi \approx 1.6 \cdot \left(\frac{T_{1\rho,\text{H}}}{T_{\text{X, aq}}}\right)^{1/2}. \quad [2]$$

The  $^1\text{H}$  decay constant under the pulsed spin-lock train,  $T_{1\rho,\text{H}}$ , is tens of milliseconds for rigid solids ( $11$ ) and a few milliseconds for mobile systems such as membrane-bound peptides ( $12\text{--}14$ ). However, samples with smaller  $^1\text{H}$  decay constants also tend to have broader  $^{15}\text{N}$  lines for the same reason of dynamics, thus the ratio in Eq. [2] may not differ as significantly for various systems. In general, the  $^{15}\text{N}$  decay constant for a static solid is almost always less than about 5 ms. Even for a very well oriented peptide, a 3-ppm resonance line at a Larmor frequency of 40.59 MHz has a decay constant of 2.6 ms. In other words, after 7.8 ms, the signal decays to 5% of the full intensity. The  $^{15}\text{N}$  acquisition time decreases even further with increasing magnetic field strengths. Assuming a  $^{15}\text{N}$  acquisition time  $T_{\text{X, aq}}$  of 4 ms, we find  $\xi = 3.5$  for  $T_{1\rho,\text{H}} = 20$  ms and  $\xi = 1.9$  for  $T_{1\rho,\text{H}} = 6$  ms. In practice, we find that an enhancement factor of roughly twofold is obtained on powder samples by the PRINS technique, in reasonable agreement with the estimated sensitivity enhancement.

## RESULTS AND DISCUSSION

The directly detected  $^{15}\text{N}$  spectrum of a powder sample of  $^{15}\text{N}$ -tBoc-Gly is shown in Fig. 2a. From the powder lineshape, an anisotropy of  $\Delta\sigma = 121$  ppm and an asymmetry parameter of  $\eta = 0.71$  were extracted, which agree well with the literature values ( $15$ ). The spectrum was acquired in 4.8 h after coadding 6144 scans. To show the noise level more clearly, the spectral region between  $-100$  and  $-250$  ppm was amplified and displayed in the inset. The signal-to-noise ratio ( $S/N$ ), calculated from the intensity of the powder maximum (71.4 ppm) relative to the 150-ppm noise range ( $-100$  to  $-250$  ppm), is 102. In comparison, the PRINS  $^{15}\text{N}$  spectrum (Fig. 2b) acquired in the same amount of time gave a  $S/N$  of 250. Thus, a 2.5-fold sensitivity enhancement was achieved by  $^1\text{H}$  detection. When comparing the signal-to-noise ratios of the two spectra, care was taken to ensure that the maximum  $t_1$  evolution time of the 2D experiment was identical to the FID acquisition time in the directly detected  $^{15}\text{N}$  experiment.

The slight deviation in the lineshape between the indirectly detected and the directly detected  $^{15}\text{N}$  spectra probably results from the orientation dependence of the additional CP step in the 2D experiment. But for the purpose of measuring the principal values of the chemical shift tensor, the  $^{15}\text{N}$  spectrum is well reproduced by the PRINS experiment. The full  $^1\text{H}$ -detected 2D spectrum is displayed in Fig. 2c, in order to illustrate the fact that the  $^1\text{H}$  signal is fully concentrated at the  $\omega_2 = 0$  cross section as a result of the pulsed spin-lock detection.

The PRINS experiment works well for the crystalline  $^{15}\text{N}$ -tBoc-Gly sample, since the  $T_{1\rho,\text{H}}$  of this compound is quite long,

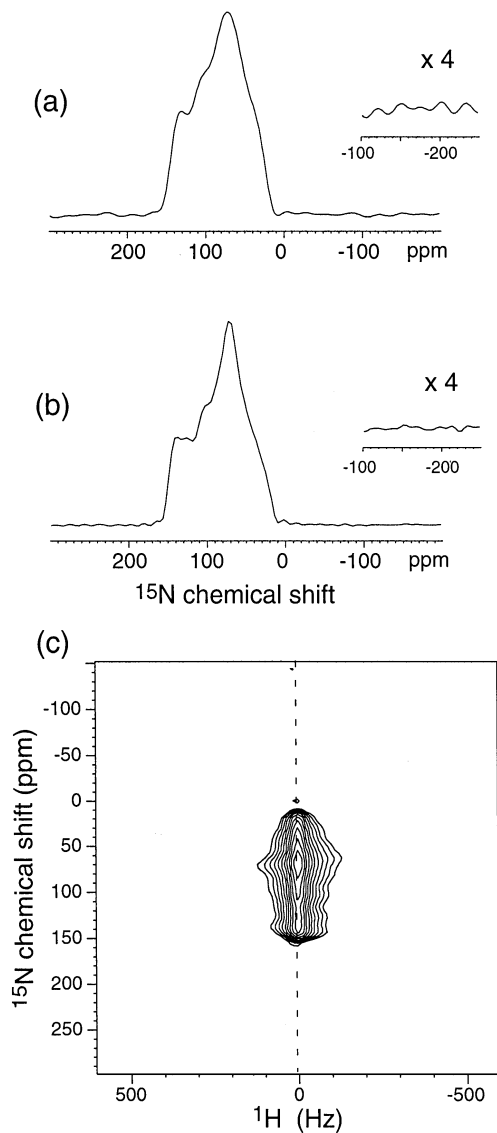


**FIG. 2.**  $^{15}\text{N}$  spectra of N-tBoc-Gly. (a)  $^{15}\text{N}$  directly detected,  $S/N = 102$ . (b)  $^1\text{H}$  indirectly detected, extracted from the cross section at the zero frequency of the  $^1\text{H}$  dimension,  $S/N = 250$ . The noise levels between  $-100$  and  $-250$  ppm are amplified fourfold and shown in the insets. Each spectrum was acquired in 4.8 h. (c) 2D PRINS spectrum, from which the 1D  $^{15}\text{N}$  spectrum (b) was extracted. The  $^{15}\text{N}$  spectra of both the directly detected and the indirectly detected experiments were processed with 10 Hz of negative exponential multiplication and 235 Hz (FWHM) of Gaussian broadening. The  $^1\text{H}$  dimension was processed with 20 Hz of exponential broadening. The maximum  $^{15}\text{N}$  evolution time was 1.6 ms, identical to the acquisition time of the 1D  $^{15}\text{N}$  experiment.

about 26 ms. A total of 5500 cycles of a  $2\text{-}\mu\text{s}$   $^1\text{H}$  pulse separated by a  $9\text{-}\mu\text{s}$  window were used, giving a total  $^1\text{H}$  acquisition time of 60 ms. In comparison, the  $^{15}\text{N}$  signal decayed in about 3 ms.

For peptides and proteins, the advantages of this  $^1\text{H}$  pulsed spin-lock detection technique are less obvious, since the  $^1\text{H}$   $T_{1\rho,\text{H}}$  of proteins, especially those associated with the lipid bilayer, tends to be shorter (14). To test the utility of the PRINS

technique for realistically sized proteins, we carried out the experiment on uniformly  $^{15}\text{N}$ -labeled and hydrated colicin Ia channel domain protein (MW = 25 kDa) in the absence of the lipid bilayer. Figure 3 compares the directly and indirectly detected  $^{15}\text{N}$  spectra of colicin Ia channel domain. The former has a maximum  $S/N$  of 41, while the latter gives a  $S/N$  of 75. This corresponds to an enhancement factor of 1.8. An enhancement was obtained despite the fact that the  $T_{1\rho,\text{H}}$  of the protein is only

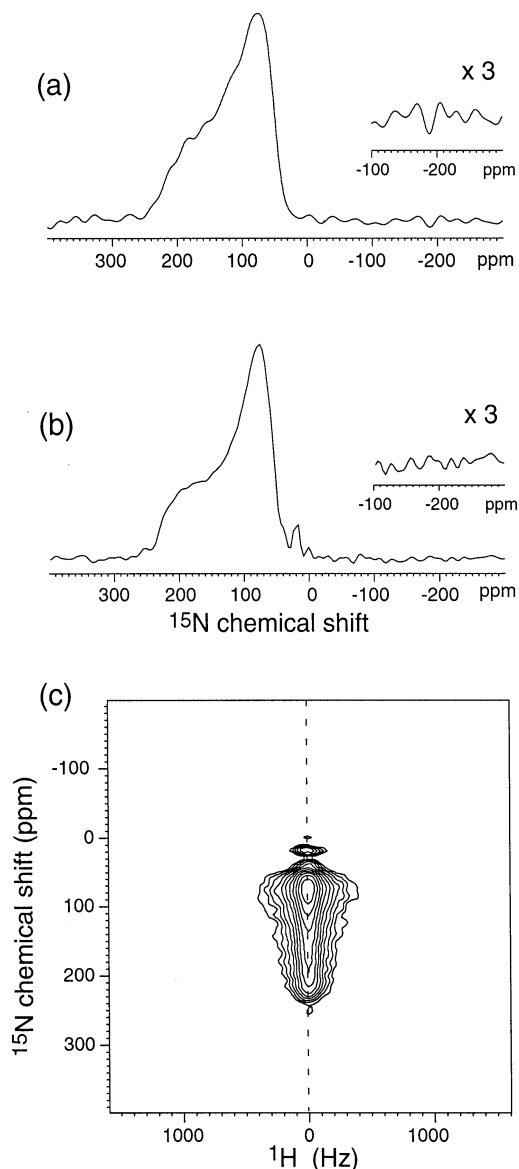


**FIG. 3.**  $^{15}\text{N}$  spectra of the colicin Ia channel domain protein. (a)  $^{15}\text{N}$  directly detected,  $S/N = 41$ . (b)  $^1\text{H}$  indirectly detected,  $S/N = 75$ . The noise levels from  $-100$  to  $-300$  ppm range are amplified threefold and shown in the insets. Each spectrum was acquired in 3.5 h. (c) 2D PRINS spectrum, from which the 1D  $^{15}\text{N}$  spectrum (b) was extracted. All  $^{15}\text{N}$  spectra were processed with 10 Hz of negative exponential multiplication and 235 Hz (FWHM) of Gaussian broadening. The  $^1\text{H}$  spectral dimension was processed with 20 Hz of exponential broadening. The maximum  $^{15}\text{N}$  evolution time was 1.6 ms, identical to the acquisition time of the 1D  $^{15}\text{N}$  experiment.

about 3 ms, which is manifested as a broader  $^1\text{H}$  line in the 2D spectrum (Fig. 3c) than that of  $^{15}\text{N}$ -tBoc-Gly. The small signal at 16.2 ppm in the PRINS  $^{15}\text{N}$  spectrum can be assigned to the  $\text{NH}_3$  groups in the protein. This resonance is in the noise level of the directly detected  $^{15}\text{N}$  spectrum, thus confirming the sensitivity improvement by  $^1\text{H}$  detection.

While the enhancement factor for colicin Ia channel domain is not large, the  $^1\text{H}$  indirect detection approach has an additional practical advantage in that it facilitates the optimization of the experimental conditions for the traditional  $^{15}\text{N}$ -detected CP experiment. The labeled model compounds used for setting up  $^{15}\text{N}$  CP experiments often have different pulse lengths from the complex proteins of interest, because these two types of systems have different conductivities and dielectric constants and thus give differential broadening of the electronic resonance of the circuit. The extremely low  $^{15}\text{N}$  signals of the proteins make it difficult to optimize the experimental conditions such as the Hartmann–Hahn match (16) and the  $^1\text{H}$  excitation pulse length directly on the sample of interest. Using the current PRINS technique, however, it becomes possible to adjust these variables directly on the proteins of interest within 8 or 16 scans by ob-

servicing the high-sensitivity  $^1\text{H}$  signals. For low-sensitivity peptides and proteins, the signal enhancement due to this improved optimization can be significant.

The same degree of sensitivity enhancement was also achieved for the 2D dipolar chemical-shift correlation experiment. Dipolar chemical-shift correlation spectroscopy, specifically  $^{15}\text{N}$ - $^1\text{H}$  dipolar and  $^{15}\text{N}$  chemical shift correlation (PISEMA), has yielded much useful information about the orientation of helical membrane peptides with respect to the lipid bilayer (3). Thus, it is of interest to examine the extent of  $S/N$  improvement achievable for these SLF spectra with the PRINS technique. The theoretical  $\xi$  for a 2D SLF spectrum by PRINS is identical to that of the 1D experiment, since only the detection of  $^{15}\text{N}$  chemical shift dimension is changed, while the  $^{15}\text{N}$ - $^1\text{H}$  dipolar dimension is recorded in the same manner in both the 2D and the 3D experiments. Figure 4 displays the 2D  $^{15}\text{N}$ - $^1\text{H}$  dipolar/ $^{15}\text{N}$  chemical shift correlation spectra of  $^{15}\text{N}$ -tBoc-Gly, obtained using the traditional SLF sequence (Fig. 4a) and with the 3D PRINS sequence (Fig. 4b). Using the integrated intensities of the area defined by the dotted lines as the criteria for sensitivity comparison, we obtain an

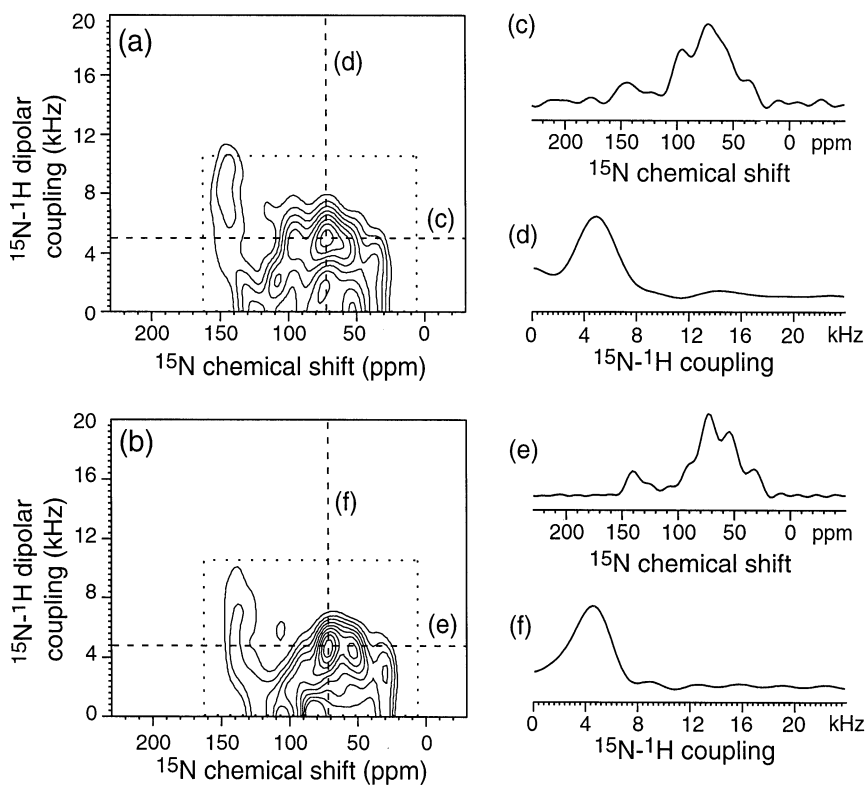


**FIG. 4.** 2D  $^{15}\text{N}$ - $^1\text{H}$  dipolar and  $^{15}\text{N}$  chemical shift correlation spectra of N-tBoc-Gly. (a)  $^{15}\text{N}$  directly detected. (b)  $^1\text{H}$  indirectly detected, extracted from the 3D data (not shown). Dotted lines define the 2D region for intensity integration and sensitivity comparison. Spectrum (b) is 2.2-fold higher in sensitivity over spectrum (a). Cross sections from the  $^{15}\text{N}$  dimension (c, e) and the dipolar dimension (d, f) at the maximal intensity of each 2D spectrum are also shown. Their  $S/N$  are: (c) 17, (d) 21, (e) 59, and (f) 23. Each experiment was conducted in 3.5 h. The  $^{15}\text{N}$  dimension and the N-H dipolar dimension of both spectra were processed with 5 Hz of negative exponential multiplication and 117 Hz (FWHM) of Gaussian broadening. The  $^1\text{H}$  dimension of the 3D spectrum was processed with 20 Hz of exponential broadening.

overall enhancement factor of 2.2 for the  $^1\text{H}$ -detected spectrum over the  $^{15}\text{N}$ -detected spectrum. Figure 4 also shows the  $^{15}\text{N}$  and  $^{15}\text{N}$ - $^1\text{H}$  cross sections of each spectrum through its highest peak. Higher sensitivities are observed for the  $^1\text{H}$ -detected spectrum in both dimensions than for the  $^{15}\text{N}$  detected spectrum.

While we used only powder samples in our demonstration of the  $^1\text{H}$  indirectly detected  $^{15}\text{N}$  static NMR, the resolutions of both the  $^{15}\text{N}$  and the  $^1\text{H}$  spectra are sufficiently high to suggest that sensitivity enhancement can also be achieved on oriented samples. Thus, this technique holds promise for sensitivity enhancement of PISEMA-type experiments as well as simple  $^{15}\text{N}$  1D experiments on membrane peptides and proteins.

The differences between the experimentally obtained enhancement factor and the theoretically estimated values result largely from the approximate nature of the parameters used in the estimate. Practically, the sensitivity enhancement by  $^1\text{H}$  detection can still be improved. For example, the  $^1\text{H}$  filling factor  $\eta_{\text{H}}$  of the RF coil may be increased by designing solid-state analogs of the inverse probes used in solution NMR. Second, a significant source of the noise in the PRINS  $^{15}\text{N}$  spectra comes from the instability of the spectrometer, since incomplete cancellation of magnetization between successive scans results in a constant offset in the time domain and thus increased noise at the zero frequency of the  $^1\text{H}$  dimension. Therefore, improving the spectrometer stability should reduce this  $t_1$  noise and increase the sensitivity of the PRINS  $^{15}\text{N}$  spectra at the  $^1\text{H}$  zero-frequency cross section.

## CONCLUSIONS

We have shown that it is possible to obtain sensitivity-enhanced static  $^{15}\text{N}$  spectra by  $^1\text{H}$  indirect detection. This is achieved by detecting the  $^1\text{H}$  signals in the windows of a pulsed spin-lock sequence, which abolishes the  $^1\text{H}$  chemical shift information in return for higher sensitivity. The  $^{15}\text{N}$  spectrum of interest is extracted as the cross section at the zero frequency of the  $^1\text{H}$  dimension. Experimental enhancement factors of 1.8–2.5 were obtained for a crystalline model compound and for a 25-kDa protein. These enhancement factors translate into a five-fold reduction in the signal averaging time, which is significant. This PRINS  $^{15}\text{N}$  NMR technique should be useful for structural studies of membrane peptides and proteins. It is also useful for optimizing directly detected  $^{15}\text{N}$  experiments, which have low sensitivity.

## EXPERIMENTAL

**Materials.**  $^{15}\text{N}$ -Labeled *N*-(*tert*-butoxycarbonyl) glycine (*N*-tBoc-Gly) was purchased from Isotec, Inc. (Miamisburg, OH) and used without further purification. About 4 mg of the powder sample was packed into the center of a 5-mm-diameter glass tube. The  $^{15}\text{N}$ -labeled colicin Ia channel domain protein (MW: 25 kDa) was synthesized as described previously (17).

A 5-mg powder sample hydrated to 30% was packed into the center of a 4-mm MAS rotor.

**NMR experiments.** All NMR experiments were carried out on a Bruker DSX-400 spectrometer (Karlsruhe, Germany) operating at a resonance frequency of 400.49 MHz for  $^1\text{H}$  and 40.59 MHz for  $^{15}\text{N}$ . The samples were placed in a high-power static probe equipped with a 5-mm solenoid coil. The pulse lengths and power levels were optimized by observing the  $^1\text{H}$  signal under the pulsed spin-lock sequence. Identical hardware connections were used for the  $^{15}\text{N}$  direct detection experiment and the  $^1\text{H}$  indirect detection experiment PRINS. The outputs of both  $^1\text{H}$  and  $^{15}\text{N}$  high-power amplifiers were connected to the preamplifier module, so that switching between  $^{15}\text{N}$  and  $^1\text{H}$  detection does not involve changing the cable connections. This ensures a fair comparison of the sensitivity of the indirect and direct detection experiments. Typical  $^{15}\text{N}$  and  $^1\text{H}$  90° pulse lengths were 6 and 3  $\mu\text{s}$ . The pulsed spin-lock sequence in the PRINS experiments consisted of 2- $\mu\text{s}$   $^1\text{H}$  pulses, which corresponded to flip angles of about 60°, separated by 9- $\mu\text{s}$  windows. Each window consisted of a 7.5- $\mu\text{s}$  delay to allow for pulse ring down and 1.5  $\mu\text{s}$  for actual data sampling. Cross-polarization contact times were 1 ms for the colicin Ia channel domain protein and 1.5 ms for *N*-tBoc-Gly, respectively. For the  $^{15}\text{N}$ - $^1\text{H}$  dipolar and  $^{15}\text{N}$  chemical-shift correlation experiment, MREV-8 was used for  $^1\text{H}$ - $^1\text{H}$  homonuclear decoupling. The  $^{15}\text{N}$  chemical shifts were referenced to the isotropic chemical shift of *N*-tBoc-Gly, which is 81 ppm relative to liquid  $\text{NH}_3$  (15).

## ACKNOWLEDGMENTS

M.H. thanks the Beckman Foundation for a Young Investigator Award. We acknowledge the Donors of The Petroleum Research Fund, administered by the American Society, for partial support of this research.

## REFERENCES

1. J. Cavanagh, W. J. Fairbrother, A. G. Palmer III, and N. J. Skelton, "Protein NMR Spectroscopy: Principles and Practice," Academic Press, San Diego, 1996.
2. Y. Ishii and R. Tycko, Sensitivity enhancement in solid state  $^{15}\text{N}$  NMR by indirect detection with high-speed magic angle spinning, *J. Magn. Reson.* **142**, 199–204 (2000).
3. T. A. Cross and S. J. Opella, Solid-state NMR structural studies of peptides and proteins in membranes, *Curr. Opin. Struct. Biol.* **4**, 574–581 (1994).
4. F. Marassi and S. Opella, NMR structural studies of membrane proteins, *Curr. Opin. Struct. Biol.* **8**, 640–648 (1998).
5. K. Schmidt-Rohr, K. Saalwachter, S. F. Liu, and M. Hong, High-sensitivity  $^2\text{H}$ -NMR in solids by  $^1\text{H}$  detection, *J. Am. Chem. Soc.*, in press (2001).
6. W. K. Rhim, D. P. Burum, and D. D. Elleman, Multiple-pulse spin locking in dipolar solids, *Phys. Rev. Lett.* **37**, 1764–1766 (1976).
7. R. K. Hester, J. L. Ackermann, B. L. Neff, and J. S. Waugh, Separated-local-field spectra in NMR, *Phys. Rev. Lett.* **36**, 1081 (1976).
8. M. G. Munowitz, R. G. Griffin, G. Bodenhausen, and T. H. Huang, Two-dimensional rotational spin-echo NMR in solids: Correlation of chemical shift and dipolar interactions, *J. Am. Chem. Soc.* **103**, 2529–2533 (1981).

9. A. Abragam, "Principles of Nuclear Magnetism," Clarendon Press, Oxford, 1961.
10. A. Pines, M. G. Gibby, and J. S. Waugh, Proton-enhanced NMR of dilute spins in solids, *J. Chem. Phys.* **59**, 569–590 (1973).
11. J. Schaefer, E. O. Stejskal, and R. Buchdahl, Magic-angle  $^{13}\text{C}$  NMR analysis of motion in solid glassy polymers, *Macromolecules* **10**, 384–405 (1977).
12. W. J. Shaw, J. R. Long, A. A. Campbell, P. S. Stayton, and G. P. Drobny, A solid state NMR study of dynamics in a hydrated salibary peptide adsorbed to hydroxyapatite, *J. Am. Chem. Soc.* **122**, 7118–7119 (2000).
13. A. Johansson, A. Wendsjo, and J. Tegenfeldt, NMR spectroscopy of PEO-based polymer electrolytes, *Electrochim. Acta* **37**, 1487–1489 (1992).
14. D. Huster, L. S. Xiao, and M. Hong, Solid-state NMR investigation of the dynamics of colicin Ia channel-forming domain, *Biochemistry*, submitted (2000).
15. T. M. Duncan, "Chemical Shift Tensors," Farragut, Madison, WI, 1997.
16. S. R. Hartmann and E. L. Hahn, Nuclear double resonance in the rotating frame, *Phys. Rev.* **128**, 2042–2053 (1962).
17. M. Hong and K. Jakes, Selective and extensive  $^{13}\text{C}$  labeling of a membrane protein for solid-state NMR investigation, *J. Biomol. NMR* **14**, 71–74 (1999).